Journal of the European Ceramic Society **10** (1992) 347–367

State of the Art

Oxygen Mobility in Silicon Dioxide and Silicate Glasses: a Review

M. A. Lamkin,* F. L. Riley§

Division of Ceramics, School of Materials, University of Leeds, Leeds LS2 9JT, UK

&

R. J. Fordham

Materials Centre, JRC Petten, 1755 ZG Petten, The Netherlands

(Received 3 July 1991; revised version received 12 November 1991; accepted 23 December 1991)

Abstract

Silicon dioxide and silicate glass films are formed on silicon nitride and silicon carbide ceramics during exposure to high-temperature oxidising atmospheres, and oxygen transport through the film is potentially a rate-controlling step. Recent published literature concerning oxygen permeation and diffusion through amorphous and crystalline silicon dioxide, and silicate glasses, is reviewed. Data for diffusion coefficients are collected to facilitate the assessment of probable dominant oxygen transport mechanisms, and associated rates, under given sets of oxidation conditions.

Bei der Auslagerung bei hohen Temperaturen und in oxidierender Atmosphäre bilden sich auf Siliziumnitrid- und Siliziumkarbid-Keramiken Glasfilme aus Siliziumdioxid und Silikat. Der Sauerstofftransport durch den Film ist hierbei möglichlicherweise ein geschwindigkeitsbestimmender Schritt. Die vor kurzem veröffentliche Literatur bezüglich der Sauerstoffpermeation und der Sauerstoffdiffusion durch amorphes und kristallines Siliziumdioxid und durch Silikatgläser wurde überarbeitet. Daten über Diffusionskoeffizienten wurden gesammelt, um die wahrscheinlich dominierende Rolle der Sauerstoff-Transport-Mechanismen und die damit verbundenen Geschwindigkeitskonstanten, bei verschiedenen vorgegebenen Oxidationsbedingungen zugänglich zu machen.

Des films amorphes de dioxide de silicium et de verre à base de silice se forment sur des céramiques à base de nitrure et de carbure de silicium aprés exposition à haute température dans des atmosphères oxydantes, et le transport d'oxygène à travers le film est potentiellement l'étape contrôlant la vitesse. De la littérature récemment publiée concernant la pénétration et la diffusion de l'oxygène à travers du dioxide de silicium amorphe ou cristallin et des verres à base de silice est passée en revue. Des données en ce qui concerne les coefficients de diffusion sont collectées pour faciliter l'estimation des mécanismes dominants probables du transport d'oxygène, ainsi que des taux associés, sous une série de conditions d'oxydation données.

1 Introduction

Silicon carbide and silicon nitride are, in common with most metals, thermodynamically unstable with respect to oxidation. The usefulness of ceramics based on these materials at temperatures in the range 1000 to 1600°C depends to a large extent, therefore, on the development of a protective oxide film. With pure materials oxidising in a clean, oxygen-containing, environment the primary oxidation product is silicon dioxide (together with gaseous carbon dioxide or nitrogen), provided the

* Present address: The Carborundum Co. Ltd, Mill Lane, Rainford, St Helens WA11 8LP, UK.
§ To whom correspondence should be addressed.

Journal of the European Ceramic Society 0955-2219/92/$5.00

oxygen partial pressure is greater than a critical value related to the stability of silicon dioxide with respect to dissociation:

$$SiO_{2(s)} = SiO_{(g)} + \tfrac{1}{2}O_{2(g)} \quad (1)$$

At 1400°C, this pressure is of the order of 10^{-5} bar.[1,2] At higher pressure a silicon dioxide layer develops. The assumption is generally made that the outwards diffusion of silicon through the silicon dioxide, leading to oxidation at the silicate–air interface, is of negligible significance, and that oxygen diffuses inwards to cause oxidation at the ceramic–silicon dioxide interface (the 'passive' oxidation reaction). Oxygen mobility in silicon dioxide tends to be low; silicon dioxide films thus provide a good barrier to the passage of oxygen, and very of possible oxidation rate-controlling processes. Very broadly speaking, oxygen mobility in silicon dioxide tends to be low; silicon dioxide films thus provide a good barrier to the passage of oxygen, and very useful lifetimes for components can be obtained. Under 'reducing' conditions of low oxygen potentials determined by equations based on eqn (1), 'active' oxidation with formation of the gaseous silicon monoxide, SiO, occurs, and faster, kinetically linear, oxidation can occur. This process will not be considered in this review.

Silicon dioxide is a complex material; it has a large number of crystallographic forms, many of which readily undergo structural rearrangement. As an 'acidic' oxide it also forms a wide range of crystalline silicates and silicate glasses. The oxidation products of technical silicon carbide and silicon nitride materials thus commonly consist of a mixture of crystalline and vitrous silicon dioxide, and crystalline or glassy silicates, depending on the composition of the starting material. The oxidation of a typical silicon nitride could, depending on the amount and nature of the sintering aid used, provide mullite, enstatite and yttrium disilicate, together with cristobalite or silica glass. Pure silicon nitride and silicon carbide yield predominantly cristobalite and silica glass. The mechanisms of oxidation of the multiphase ceramics can also be complex, but a basic assumption is that a degree of protection is provided by a thin silicon dioxide layer at the ceramic–oxide interface.[3-5] For this reason it is of interest to examine published data relating to oxygen mobility in silicon dioxide. Because of the almost inevitable contamination (by impurities and sintering aids) of oxidation systems this survey can be usefully extended to include silicate glasses. Self-diffusion of oxygen and metal cations in crystalline silicates is a related subject but beyond the scope of this review. Comprehensive data surveys have been published on other simple and binary oxides,[6-7] minerals[8] and glasses.[8-9]

2 Silicon Dioxide

2.1 The phases of silicon dioxide

Under 1 bar pressure, three crystalline forms of silicon dioxide,[10] quartz, tridymite and cristobalite, are stable. Each phase has a high–low inversion between polymorphs, normally referred to as α- and β-forms. Transformation temperatures are shown schematically in Fig. 1.

The low-temperature inversions between the α- and β-forms are rapid, involving only a slight alteration to the crystal structure, whereas transformations between major crystalline forms are sluggish, since they require the breaking of bonds. The conversion of tridymite or cristobalite to quartz below 867°C is so slow that in practice it is never seen. On cooling liquid silicon dioxide below 1710°C crystallisation is not normally accomplished without either long annealing times or the addition of suitable stabilisers, so that silica glass is usually produced. Table 1 gives crystallographic data for the principal forms of silicon dioxide.

Silica glass and the three most common crystalline forms of silicon dioxide are constructed from SiO_4 tetrahedra with an oxygen atom at each corner and a silicon atom at the centre. Each oxygen atom is shared by two tetrahedra, giving an O–S–O bond angle of ~109°. The interatomic distances are Si–O (158 pm), O–O (260 pm) and Si–Si (320 pm).[11] The differences between the phases arise from the manner in which the tetrahedra are arranged, with a variation in the Si–O–Si bond angle.

Quartz, the low-temperature phase, is stable up to 870°C. It has not been reported as an oxidation product of silicon nitride or silicon carbide.

Tridymite is the most complex and least well understood of the three crystalline phases and has a number of crystallographic modifications. The stable phase is the S-type (metastable below 867°C), which has six modifications. The three low-temperature S-type modifications (S_I, S_{II}, S_{III}) are all orthorhombic and differ only slightly from each other, and are for convenience collectively referred to as low or α-tridymite (α_1, α_2, α_3). Likewise, the three higher-temperature hexagonal forms (S_{IV}, S_V, S_{VI}) are commonly referred to as high or β-tridymite (β_4, β_5, β_6). There is also a metastable form (M-type), with three minor modifications, which slowly (appreciably above ~1000°C) transform to one of

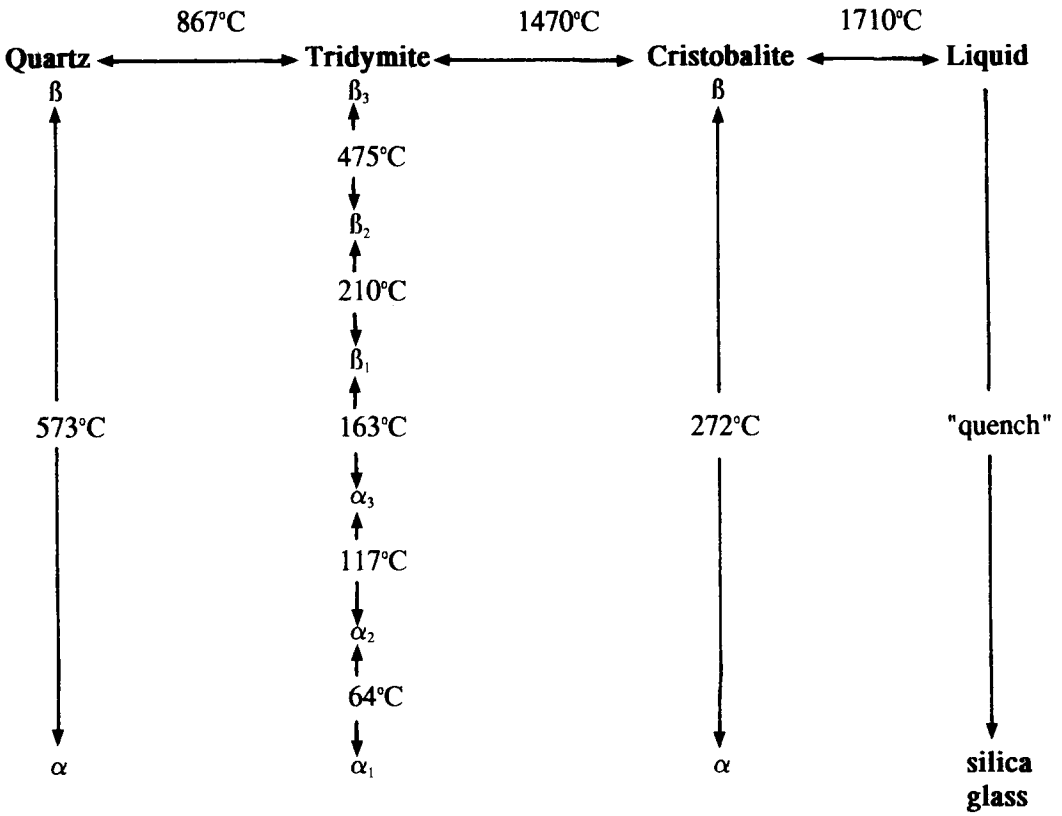

Fig. 1. 'Stable' phase relations of silicon dioxide.

the six modifications of the S-type. There is also a short-lived unstable form (U-type). Tridymite slowly transforms to cristobalite above 1470°C, but the transformation to quartz below 867°C is not observed.

Tridymite has the most open structure of the three main crystalline forms with more than 50% void in the unit cell. It is capable of taking up to 9 mol% of sodium ion into its structure.[10,13] Tridymite shows variance with the normal rule that higher-temperature stable polymorphs have the most open, and lowest density, structures. 'Chemically pure' tridymite is never observed and it always appears to contain a small amount of other oxides. A number of investigators have thus claimed that tridymite is not a true phase of silicon dioxide, but a solid solution of silicon dioxide with other oxides.[14-16] In addition, the direct conversion of quartz to cristobalite has been observed at ~1050°C,[15,16] subsequently proposed for the 'quartz–cristobalite transformation' temperature. Other workers, however, have presented evidence which appears to show increased

Table 1. Crystallography of silicon dioxide

Phase	*ρ* ($Mg\,m^{-3}$)	*Crystal symmetry and unit cell dimensions (pm)*	*Si–O–Si bond angle* (°)	*Largest structural void radius (pm)*	*Percentage void in unit cell*[a]
α-Quartz	2·65	Rhombohedral, $Z = 3$, $a = 490$, $c = 539$	144	—	38·1
β-Quartz	2·60	Hexagonal, $Z = 3$, $a = 501$, $c = 547$	146	100	40·8
α-Tridymite	2·27	Orthorhombic, $Z = 64$, $a = 988$, $b = 1710$, $c = 1630$	140	—	54·1
β-Tridymite	2·30	Hexagonal, $Z = 4$, $a = 503$, $c = 822$	—	130	51·7
α-Cristobalite	2·33	Tetragonal, $Z = 4$, $a = 496$, $c = 692$	148	—	45·3
β-Cristobalite	2·21	Cubic, $Z = 8$, $a = 712$	152	170	48·4
Silica glass	2·20	—	120–180 Mean = 144	—	57[b]

[a] Percentage void calculated on a basis of Si^{4+}, O^{2-} and N^{3-} radii of 41, 140 and 170 pm, respectively.
[b] See Ref. 11.
Z = Number of SiO_2 units per unit cell.

stability of tridymite with increasing purity, and consequently it has been argued that tridymite is indeed a true polymorph of silicon dioxide.[17-19] Although there remains uncertainty over the nature of tridymite, it appears clear that a mineraliser (such as an alkali metal oxide) greatly assists its formation.

Cristobalite, the phase stable above 1470°C up to the melting point at 1710°C, can exist (metastably) below 1470°C. The low-temperature modification, α-cristobalite, is tetragonal and rapidly converts to the cubic β-form above 270°C. Polycrystalline critobalite has a characteristic curved ('fish-scale') fracture surface.[20,21] As in tridymite, the crystal structure is an open one with the atoms occupying 48·4% of the space in the β-form, and is capable of taking up to 4 mol% of sodium ion into its structure.[10] An unstable form of cristobalite is the D-type with a disordered crystal structure, and which usually forms as an intermediate phase during transformation between polymorphs.

Liquid silicon dioxide normally forms silica glass on cooling. Structural rigidity of a glass is associated with a steady increase in viscosity with decreasing temperature. On continuous cooling there is an abrupt change in certain properties (notably the specific volume) over a small temperature range. This range is referred to as the glass transition temperature θ_g. For pure silica glass, $\theta_g = 1100$–1150°C.[22] Above θ_g, the material is usually termed a *supercooled* or *glass-forming liquid*; below this temperature it is termed a *glass*. This behaviour is illustrated in Fig. 2.

Silica glass has been comprehensively reviewed.[10,12,23] The structure is usually described by the 'random network' hypothesis[24] which envisages the random arrangement of tetrahedra formed by the variation of the Si–O–Si bond angle. This angle

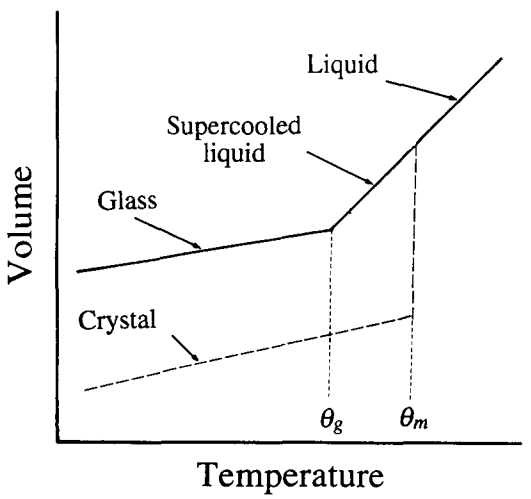

Fig. 2. Volume as a function of temperature for glass and crystal forms. θ_g = glass transition temperature; θ_m = melting point.

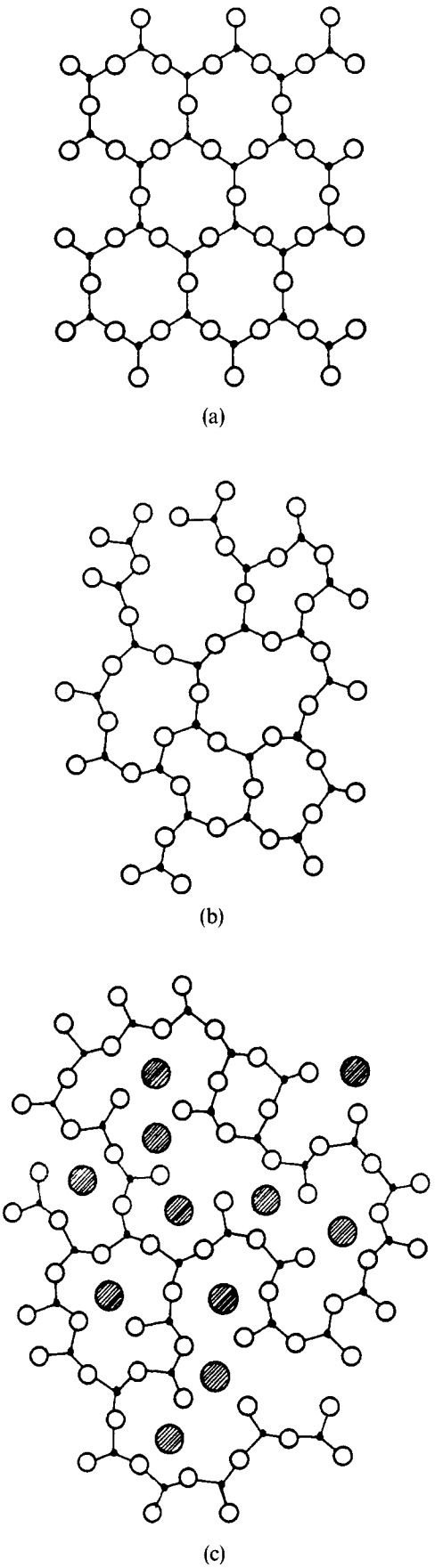

Fig. 3. Two-dimensional representation of the crystal structure of (a) crystalline SiO_2; (b) silica glass, after Zachariasen;[24] (c) sodium silicate glass, after Warren & Biscoe.[25] ●, Na^+; ○, O^{2-}; •, Si^{4+}.

Table 2. Classification of commercial silica glasses[12a]

Type	*Production method*	*Impurity concentration (ppm)*	
		Metallic	*Hydroxyl ion*
I	Electrical fusion of quartz	50–300	5–15
II	Flame fusion of quartz	< type I	100–500
III	Hydrolysis of $SiCl_4$ in $O_2 + H_2$ flame	< 1	900–1 300 (+ ~ 100 Cl)
IV	Hydrolysis of $SiCl_4$ in water vapour-free plasma flame	< 1	< 2 (+ 200–800 Cl)

can vary from 120 to 180° with a mean value of 144°. Thus, the three-dimensional structure lacks the long-range order of a crystalline solid but possesses the short-range order of the SiO_4 tetrahedra. Figure 3 gives a two-dimensional representation of crystalline and amorphous materials to illustrate this model.

Commercially available silica glass is usually classified according to its method of manufacture. The system proposed by Bruckner[12a] is summarised in Table 2. Types I and II silica glasses are commonly referred to as 'natural silica' because they are formed from quartz, whereas types III and IV are called 'synthetic silica'. Silica glass produced by the oxidation of silicon is believed to differ from commercial silica by having structural channels that form parallel to the growth direction.[26–30] These channels are similar to those along the *c*-axis in *β*-quartz and *β*-tridymite,[26] and can act as fast diffusion paths for molecular species.[27]

2.2 Silicate glasses

The addition of one or more oxide components to silica glass makes a significant difference to the structure and properties of the material.[31] Oxides, in the context of glass formation, can broadly be subdivided into three classes:

(i) *Network formers* which are essential to development of the glass structure. By far the most common is SiO_2, but the class also includes B_2O_3, GeO_2, As_2O_3 and P_2O_5.

(ii) *Network modifiers* such as Na_2O, K_2O, Li_2O, MgO, CaO and Y_2O_3 which disrupt the continuity of the glass structure by breaking bonds with the formation of non-bridging oxygens (as shown in Fig. 4(c)). Monovalent ions will form one non-bridging oxygen per cation, and divalent ions will form two non-bridging oxygens. The cations are located in interstices in the glass structure—the size of the ion determining the size of the hole it can ocupy. Smaller ions tend to have higher mobilities than larger ions. According to the random network theory[24] the cations should be distributed randomly and fairly homogeneously throughout the network. However, evidence does exist to indicate that cations may be grouped in pairs, and as clusters.[32,33]

(iii) *Intermediate oxides* such as Al_2O_3, BeO, TiO_2 and ZrO_2 which, although they cannot in normal conditions form glasses by themselves, in some circumstances enter glass and modify its structure. The replacement of Si^{4+} by Al^{3+} requires an additional monovalent (or fractional polyvalent) cation to occupy an adjacent structural 'hole' to preserve charge neutrality.

2.3 Phase transformations in silicon dioxide

The devitrification (crystallisation) of silica glass, and the transformation of one silicon dioxide phase to another have received much attention.[10,13–19,34–41] As a general rule, phase transformations are facilitated by the presence of liquids. Transformation follows typical 'C'-shaped kinetics with the rate showing minima at the extremes of the temperature stability field, and a maximum near the middle. Tridymite formation is favoured by monovalent metal ions[35–38]—Li^+, Na^+ and K^+; divalent ions favour cristobalite.[35] The power of the mineraliser to promote crystallisation is dependent on the ionic radius in the order $Li^+ > Na^+ > K^+$ (ionic radii 78, 90 and 133 pm, respectively). Increasing concentrations of alkali increase the transformation rate, although a saturation limit is reached above which increased concentration has no further effect. D-Cristobalite is usually the first phase formed, and is then redissolved in the liquid, from which the stable silicon dioxide form subsequently crystallises.[13,38–41]

3 Oxygen Mobility in Silicon Dioxide, Amorphous Silica and Silicate Glasses

3.1 Introduction

The mobility of an atom or molecule can be treated in terms of Fick's first law:

$$J = -D\frac{dC}{dx} \tag{2}$$

where J is the flux of a species diffusing through a plane normal to the concentration gradient dC/dx,

with a diffusion coefficient D. Diffusion is a thermally activated process, and the diffusing species must overcome an energy barrier. D is thus related to temperature T, by an Arrhenius-type equation:

$$D = D_0 T^n \exp\left(\frac{-\Delta H^{\ddagger}}{RT}\right) \quad (3)$$

where $\Delta H^{\ddagger}$ is the activation enthalpy, D_0 the pre-exponential constant or frequency factor, R the gas constant, and n a temperature dependence exponent. For simplicity, the pre-exponential T term is normally ignored ($n = 0$), since, compared with the exponential T term, it has only a small influence on the mobility. Most diffusion data are presented in terms of D_0 and $\Delta H^{\ddagger}$, so allowing the ready calculation of mobilities at different temperatures.

For diffusion of a gas across a membrane of thickness d, the flux is given by:

$$J = -P\frac{(p_1 - p_2)}{\mathrm{d}p^0} \quad (4)$$

where p_1 and p_2 are the vapour pressures on each side of the membrane, p^0 is the standard pressure, and P is a constant referred to as the permeability constant. Permeation and diffusion, although related, are not the same process. Permeation is the overall steady-state diffusional flow of solute across a membrane driven by an external pressure gradient, whereas diffusion is the internal movement of individual atoms or molecular species from one structural point to another. Assuming D to be independent of concentration, permeation and diffusion are related by the expression:

$$P = DS \quad (5)$$

where S is the solubility of solute in the solvent (O_2 in SiO_2 for example) under the conditions of the study. For the purposes of this review, the term 'permeation' will be used for the flow or 'diffusion' of a molecular species through a material with little or no chemical interaction with the lattice. The solubility term S is thus the physical solubility. The term 'diffusion' will be used to mean the self-diffusion of network oxygen.

3.2 Oxygen mobility in amorphous silicon dioxide

Species able to diffuse in silica glass can be subdivided into three categories:

(a) Those which are inert, e.g. helium.
(b) Those which can disrupt the structure, e.g. sodium ions.
(c) Those which can substitute into the structural network of a glass, e.g. aluminium ions.

In some cases it can be difficult to identify the diffusion mechanism when the diffusing species category is uncertain. As will be seen, the diffusion of oxygen in silica glass can be fitted to categories (a) or (c), depending on the nature of the oxygen species and the conditions.

There are, in principle, two basic routes available for oxygen migration in crystalline and amorphous silica (and related silicate glasses):

(a) The channels of open space in the low density structures, permitting permeation of molecular oxygen by relying on the physical solubility of oxygen in the solid.
(b) The network of bonded oxygens through which structural oxygen self-diffusion can occur by making use of what in a crystalline structure would be identified as lattice vacancies, or interstitial positions, and involving the breaking and reforming of bonds.

If the two oxygen transport processes operated entirely independently, process rates would be relatively easy to measure in terms of overall molecular oxygen movement through the structure, or of isotopic exchange with the network oxygens. However, because silica and the silicate glasses can dissolve appreciable quantities of molecular oxygen, the two oxygen transport processes can, in principle, become interlinked, and it has been proposed that internal interchange between dissolved molecular oxygen (acting in effect as an 'interstitial' defect) and network oxygen can occur. This leads to a third mechanism for oxygen transport, termed 'interstitialcy diffusion'. As a consequence it is necessary to distinguish between the results of isotopic exchange measurements carried out in the presence of gaseous oxygen, and those carried out in the complete absence of the gas phase. The three processes are illustrated schematically in Fig. 4.

Published data for the diffusion of molecular and atomic oxygen in silica glass[22,42–49] are summarised in the Appendix in Table A1 and Fig. A1.

3.2.1 Permeation

Norton[42] alone has reported values of D obtained from measurements of the permeation of molecular oxygen through silica glass. A mass spectrometer was used to measure gas flow through the thin membrane of a silica glass bulb. The rate of oxygen permeation was measured directly to give P_{O_2}, and the diffusion coefficient D_{O_2} (the diffusivity of molecular oxygen through silica), calculated by the lag-time method, where D_{O_2} is related to the time

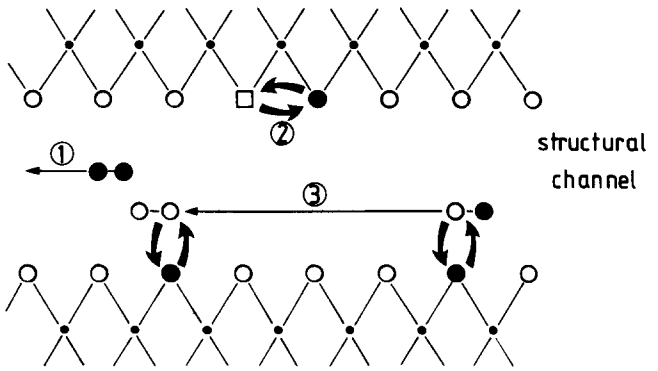

Fig. 4. Schematic representation of oxygen transport mechanisms in silica glass. 1, Molecular permeation through internal channels; 2, exchange between network oxygen and network vacancy; 3, interstitialcy diffusion: exchange between network oxygen and molecular oxygen present either within the internal channels, or at an external surface. ○, ●, Oxygen atoms; □, oxygen vacancy; ●, silicon atom.

taken to establish a steady flow of oxygen. D_{O_2} over 950–1078°C fits the equation:

$$D_{O_2} = 2{\cdot}7 \times 10^{-8} \exp\left[\frac{-113\,\text{kJ mol}^{-1}}{RT}\right] \text{m}^2\,\text{s}^{-1} \quad (6)$$

Using eqn (5), oxygen solubility at 1078°C was determined to be $1{\cdot}9 \times 10^{-3}$ cm^3 O_2/cm^3 SiO_2. Norton gives two values of the activation enthalpy for permeation: 92 kJ mol^{-1},[42a] and 112 kJ mol^{-1}.[42b] The value of the activation enthalpy for diffusion is similar to that of 131 kJ mol^{-1} determined earlier by Barrer,[50] from measurements of gas flow rates obtained by recording the change of pressure across a silica glass membrane.

Oxygen is generally believed to permeate through silica glass as the molecular species O_2.[51,52] Several workers[43,45,53–55] have reported a linear pressure dependence for oxygen diffusion, implying that O_2 is the diffusing species and not monoatomic oxygen vacancies or ions, the concentrations of which are not linearly dependent on p_{O_2}. The activation enthalpy of ~110 kJ mol^{-1} would be low for a mechanism involving bond breaking. This view is broadly supported by the use of ^{18}O as a tracer to follow oxygen migration through silica films formed by ^{16}O oxidation of silicon,[49,56–61] showing a high concentration of ^{18}O at the Si–SiO_2 interface but a low concentration of tracer in the bulk of the oxide, as shown schematically in Fig. 5. This implies a low level of exchange between the permeating O_2 and the lattice oxygen, again suggesting a molecular permeation process. At 1300°C, however, ^{18}O tracer is more evenly distributed throughout the oxide,[57] as a result of appreciable exchange between network and interstitial O_2.[48] The dominant migration mechanism thus changes with temperature, an expected

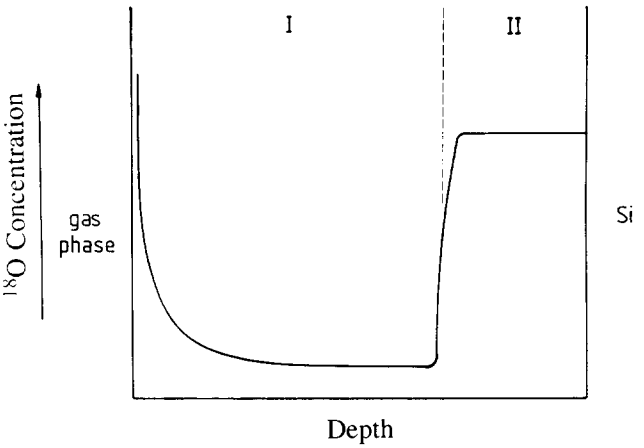

Fig. 5. Schematic representation of ^{18}O tracer diffusion profile across a SiO_2 film, initially grown using $^{16}O_2$, then $^{18}O_2$.

feature of processes with different activation enthalpies. Tracer studies generally show a high level of oxygen exchange close to the oxide–atmosphere interface. This can be explained if it is assumed that oxygen exchange occurs more readily where there are broken Si–O bonds, the concentration of which at the external surface is clearly higher than that within the internal diffusion channels.

It has been assumed that the activation enthalpy for permeation in silica glass is proportional to the strain energy S_E required to deform the diffusion channels by stretching the bonds sufficiently to accommodate an incompressible molecule.[62] On this basis, the strain energy S_E is given by the equation:

$$S_E = 8\pi G r_D (r - r_D)^2 \quad (7)$$

where G is the elastic modulus of the glass, r_D the radius of the diffusion channel and r the radius of the diffusing molecule. Thus the square root of the activation enthalpy should be proportional to the radius of the molecule. Figure 6 shows $\Delta H^{\ddagger 1/2}$ as a function of r for data for molecular (or atomic) diffusion through silica glass over the temperature range 700–1200°C. The straight line fit for these data indicated good agreement with this model. Extrapolating to zero enthalpy gives a diffusion channel diameter of 85 pm. A value of 110 pm has been determined by incorporating a pre-exponential T term in eqn (3).[63]

3.2.2 Oxygen self-diffusion in the absence of gaseous oxygen

In the absence of a suitable radio-isotope tracer, self-diffusion measurements make use of the stable isotopes, ^{17}O or (more commonly) ^{18}O, with the amount and distribution of oxygen tracer followed by mass spectrography, SIMS, or by means of

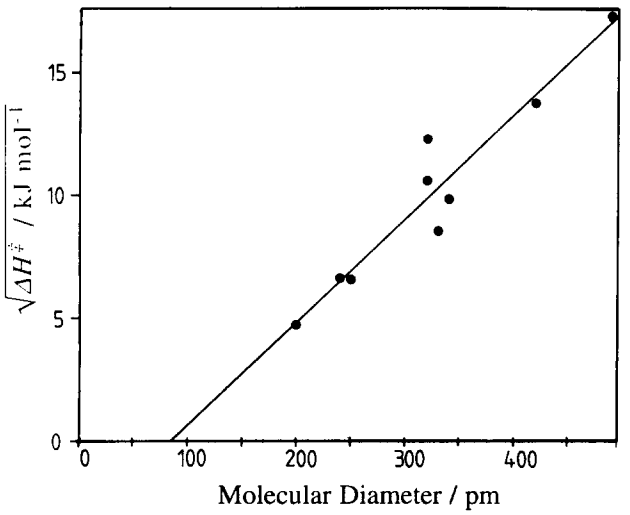

Fig. 6. $\Delta H^{\ddagger 1/2}$ as a function of molecular diameter for gas permeation through silica glass.

nuclear reactions. Because of the, at least theoretical, possibility of interchange between molecular oxygen and network oxygen, measurements of oxygen self-diffusion in the absence of dissolved molecular oxygen become important. Mikkelsen[49] has used SIMS to profile the extent of oxygen self-diffusion between two thin (~150 nm) silicon dioxide films formed by chemical deposition from the reaction of N_2O and silane, one of which was enriched with ^{18}O tracer. Diffusion was thus carried out under conditions preventing access of gaseous oxygen to the films. D^*_O is given by:

$$D^*_{O(1200\text{–}1400\,^\circ C)} = 2{\cdot}6 \times 10^{-4} \exp\left[\frac{-450\,\text{kJ mol}^{-1}}{RT}\right] \text{m}^2\,\text{s}^{-1} \quad (8)$$

It may be significant that this activation enthalpy value is close to that of the Si–O bond energy (440 kJ mol^{-1}).

3.2.3 Oxygen self-diffusion involving gaseous oxygen exchange

Network oxygen self-diffusion has been most frequently studied by the method of heterogeneous isotope exchange. The silica specimen is surrounded by oxygen enriched with the isotopic tracer and the degree of isotope exchange is measured. If the migration of gas to the solid–gas interface and subsequent exchange at the interface are assumed to be fast, the rate-controlling process is the inter-diffusion of ^{18}O and ^{16}O within the Si–O network; and diffusion rates can be determined.

A number of workers report data for the self-diffusion of network oxygen D^*_O by this method.[22,43–47] The most reliable data are generally considered to be those of Williams,[45] Muehlenbachs & Schaeffer,[22] Yinnon[46] and Kalen *et al.*[47] The first three are expressed, respectively, by the following equations:

$$D^*_{O(850\text{–}1250\,^\circ C)} = 2{\cdot}1 \times 10^{-13} \exp\left[\frac{-121\,\text{kJ mol}^{-1}}{RT}\right] \text{m}^2\,\text{s}^{-1} \quad (9)$$

$$D^*_{O(850\text{–}1250\,^\circ C)} = 4{\cdot}4 \times 10^{-15} \exp\left[\frac{-82{\cdot}5\,\text{kJ mol}^{-1}}{RT}\right] \text{m}^2\,\text{s}^{-1} \quad (10)$$

$$D^*_{O(706\text{–}1018\,^\circ C)} = 2{\cdot}1 \times 10^{-14} \exp\left[\frac{-111\,\text{kJ mol}^{-1}}{RT}\right] \text{m}^2\,\text{s}^{-1} \quad (11)$$

Other data[43,44] are considered to be unreliable because of phase boundary effects between the material and the atmosphere, and because of the short times over which diffusion was allowed to take place.[22,45,53]

Kalen *et al.*[47] used SIMS to profile ^{18}O tracer diffusion and assumed two independent diffusion processes—network and interstitial. For network diffusion D^*_O is given by:

$$D^*_{O(800\text{–}1200\,^\circ C)} = 5{\cdot}54 \times 10^{-15} \exp\left[\frac{-143\,\text{kJ mol}^{-1}}{RT}\right] \text{m}^2\,\text{s}^{-1} \quad (12)$$

Figure A1 in the Appendix shows that this equation gives values for D^*_O of the same order as that of Mikkelsen[49] for network oxygen diffusion in the absence of interstitial O_2 (in spite of a different activation enthalpy). Muehlenbachs & Schaeffer's[22] diffusivity value at 1012°C, which does not fit their own eqn (9), is consistent with eqn (12). Muehlenbachs & Schaeffer suggested that the value at 1012°C did not fit their eqn (9) because, unlike their other datum points, it was below the glass-transition temperature (θ_g). However, it has been suggested by Kalen *et al.*[47] that at this temperature Muelenbachs & Schaeffer might not have achieved significant exchange between the network and the interstitial oxygen (although other workers apparently had little problem at lower temperatures) and that they were measuring the network diffusivity as given in eqn (11).

Activation enthalpies for the network self-diffusion process determined by isotope exchange experiments (85–121 kJ mol^{-1}) are thus broadly similar to the value for molecular diffusion (113 kJ mol^{-1}), suggesting a related transport mechanism. D^*_O has also been found to be linearly dependent on the oxygen partial pressure.[45] On this

basis, and as the activation enthalpy is much smaller than the Si–O bond energy, Schaeffer[64] has proposed an 'interstitialcy diffusion' mechanism, requiring the presence of O_2, for the self-diffusion of oxygen in silica glass. Oxygen self-diffusion was assumed to proceed by the exchange of network oxygen with interstitially dissolved O_2; that is, molecular oxygen acts as an interstitial defect or 'carrier' for the network oxygen[43,64,65] (mechanism 3 of Fig. 4). Additional evidence for this mechanism comes from data[27,53,64] which appear to confirm an equation of Haul & Dumbgen,[43] showing a link between D_{O_2} and D_O^*:

$$D_{O_2} c_{O_2} = D_O^* c_O \tag{13}$$

Further support for the validity of this model is provided by the work of Deal & Grove,[55] who have derived an expression for the parabolic rate constant for silicon oxidation by molecular oxygen as a function of the diffusion coefficient for oxygen in the developing oxide film:

$$kp = 2D \frac{C_{O_2}}{C_O^*} \tag{14}$$

From eqn (13) this gives[64]

$$kp = 2D_O^* \tag{15}$$

This relationship is confirmed by direct comparisons of measured kp and D_O^* values[64] provided the thermally grown silicon dioxide films have reached 'thick' film dimensions ($\geq \mu$m). For 'thin' films of nm dimension linear kinetics are seen, because of ordering in the oxide structure. Values of D_O^* obtained using eqn (14) are about three times larger than those measured by Norton;[42] this is normally explained by assuming that oxygen diffusion occurs preferentially along structural channels in the silicon dioxide film.[27] However, Cawley *et al.*[60] point out that if the 'interstitialcy diffusion' mechanism applied to silica glass, the ^{18}O concentration in tracer diffusion studies would be significant throughout the oxide and not seen merely at the gas–solid interface, as is the case, at least in the lower-temperature region. They conclude that eqn (13) is not valid, and that experimental evidence that supports it is merely coincidental. It has also been argued[65] that because of $^{18}O \leftrightarrow {}^{16}O$ exchange at or near to the gas–oxide interface, the concentration of $^{18}O_2$ (and $^{18}O^{16}O$) in the permeating O_2 is very much smaller than the concentration of $^{18}O_2$ at the oxide. Thus, ^{18}O exchange with the network oxygen is negligible and below the detection limit of SIMS.

An empirical method for comparing independently determined kinetic data is to plot the logarithm of the pre-exponential factor as a function of the activation energy. Such treatment has arisen from the observation that for a range of data the pre-exponential factor tends to increase with increasing activation enthalpies. Data arising from the same mechanism tend to lie on a straight line. This relation is known as the compensation law (Meyer–Neldel rule or isokinetic effect)[66,67] and is expressed:

$$\ln D_O = \alpha \Delta H^{\ddagger} + \beta \tag{16}$$

where α and β are constants. A number of thermally activated processes obey this law, such as conductivity in semiconductors,[66] heterogeneously catalysed reactions[68] and diffusion in solids and glasses.[67,69–73] Figure 7 shows the good agreement with the compensation law of permeation-assisted oxygen self-diffusion in silica glass, but suggests that differences in mechanisms exist for pure network self-diffusion (Kalen *et al.*[47] and Mikkelsen[49]), and for pure permeation.[42]

3.3 Oxygen mobility in crystalline silicon dioxide

Most work on the mobility of oxygen in crystalline forms of silicon dioxide has involved studies of hydrothermal diffusion in mineral quartz.[74–77] However, there are some data from heterogeneous isotope exchange experiments for oxygen self-diffusion in quartz using ^{18}O tracer under 'dry' conditions; the activation enthalpies of 230 kJ mol^{-1}[43] and 195 kJ mol^{-1}[78] are much larger than the values for silica glass. An activation enthalpy of 195 kJ mol^{-1} has been determined for oxygen self-diffusion in tridymite.[78] There are no data for oxygen exchange in cristobalite, but four widely differing values obtained from oxidation studies on silicon carbide and silicon nitride powder

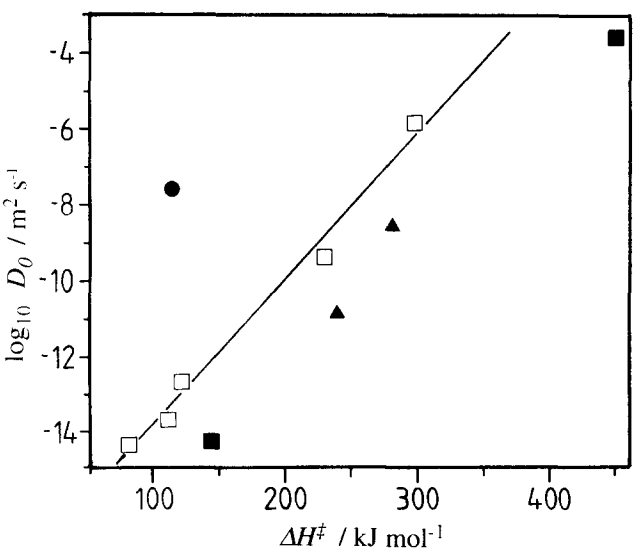

Fig. 7. $\log D_O$ as a function of $\Delta H^{\ddagger}$ for oxygen diffusion in silica glass. ●, O_2 permeation after Norton;[42a,b] ■, self-diffusion after Kalen *et al.*[47] and Mikkelsen;[49] ▲, network diffusion at SiO_2–Si and SiO_2–gas interfaces after Cawley & Boyce.[48]

have been published, where the reaction rate was assumed to be controlled by oxygen diffusion through a protective cristobalite layer.[79-81] Doubt exists over the validity of these results because no account was taken of preferential diffusion along polycrystalline cristobalite grain boundaries, or of powder purity.

Oxygen diffusion data for crystalline silicon dioxide are summarised in the Appendix in Table A2 and Fig. A2. Although there is much scatter, it is clear that the rates of diffusion of oxygen in crystalline silicon dioxide are slower than in silica glass. The similarity in the densities of silica glass, β-tridymite and β-cristobalite (2·20, 2·30 and 2·21 $Mg\,m^{-2}$, respectively) indicates similar open structures. Hence it seems reasonable to suppose that similar oxygen transport mechanisms exist for these materials, with rates modified by slight structural variations. As discussed in Section 2.2, silica glass is composed of rings with varying numbers of SiO_4 tetrahedral components. Migration of molecular oxygen will occur preferentially through the larger seven-, eight-, nine-, etc., membered rings. Cristobalite and tridymite contain similar rings, but each ring has only six-member units. Thus, the diffusion channels in crystalline silicon dioxide are smaller in size than the mean of those in silica glass, and the energy barriers for migration in crystalline silicon dioxide would be expected to be larger. No comparative work has been carried out using oxygen, but helium and neon[82,83] have been found to permeate under comparable conditions through tridymite and cristobalite at slower rates than through silica glass; activation enthalpies for crystalline silicon dioxide are approximately twice those of silica glass. Since the solubility and permeation rate of neon in cristobalite are so small (virtually undetectable),[82] it is unlikely that molecular oxygen will have an appreciable permeation rate.

Gas pressure dependences have not been reported for oxygen diffusion in crystalline silicon dioxide; if molecular oxygen were the migrating species, then a linear dependence of rate on pressure would be expected because it is solubility controlled.

3.4 Oxygen mobility in silicate glasses and liquids

This subject must differentiate not only between permeation and self-diffusion, but also between migration taking place within a glass (the temperature below θ_g) and in a liquid (above θ_g).

3.4.1 Permeation in glasses (below θ_g)

Gas mobility is dependent on the size of the diffusing species and the accessible free volume in the glass.[84] Thus gas mobility is controlled not only by the concentration of network formers or modifiers, but also by the effect of these on the glass structure. No work has been published on the effect of oxide additions to silica glass on oxygen permeation: however, the helium permeation rate increases with increasing R–O–R′ bond length ($R = SiO_4^{4-}$, $R' = TiO_4^{4-}$, for example),[85,86] and thus with increasing effective diameter of the permeation channel path; a similar effect would be expected for oxygen.

The effect of Na_2O and K_2O additions on helium permeation in silica glass has also been studied.[87,88] The Na^+ and K^+ cations are located in the interstices (Fig. 3), which form the diffusion channels. Gas permeation is affected in two ways: firstly, the diffusing gas molecule must go round the obstructing ion, so increasing the diffusion path length; secondly the free volume for permeation is reduced. Both factors would result in slower permeation rates (indeed, permeation rates may be reduced to the extent that the contribution made by oxygen self-diffusion to the overall oxygen transport process becomes dominant).

3.4.2 Self-difusion in glasses (below θ_g)

Self-diffusion coefficients for oxygen in silicate glasses (that is, at temperatures below the glass transition temperature) have been determined using similar techniques to those used for permeation-assisted self-diffusion in silica glass. Much of the work has concentrated on soda–lime–silica (SiO_2–CaO–Na_2O) glasses and the $40SiO_2$–40CaO–$20Al_2O_3$ slag composition, but a wide range of other glasses has been studied. The low activation enthalpies seen have led to the suggestion that the diffusion mechanism is unlikely to involve viscous flow or bond breaking, and that diffusion of molecular oxygen occurs.[89,90] An alternative mechanism involving 'quenched in' defects in the glass has been proposed,[91] for which a low pre-exponential factor is considered to indicate a small defect population, and a low activation enthalpy a low energy barrier to movement. The migration energy ΔH_m is calculated from the expression:[92]

$$\Delta H_m = 8m\lambda^2 v^2 \qquad (17)$$

where m is the mass of the diffusing atom, λ the mean jump distance, and v the vibrational frequency of a particle in a potential well. v, given by Lindemann's equation,[93] was originally determined for crystals:

$$v = b\sqrt{\frac{T_g}{AV_A^{2/3}}} \qquad (18)$$

where T_G is the glass transition temperature, A the atomic mass and V_A the atomic volume, and b (a constant) $= 2{\cdot}8 \times 10^{12}\ s^{-1}\ m^{-1}\ K^{-1/2}$. The values of ΔH_m calculated from this model are in fair agreement with those determined experimentally.

3.4.3 Oxygen mobility in silicate liquids (above θ_g)
Oxygen migrates through a liquid silicate relatively quickly, and the mechanism is modelled as that of a molecule moving through channels in the liquid. The self-diffusion of oxygen in liquids is less well-understood and several mechanisms have been proposed. The first widely used theory is based on the Stokes' equation:

$$B = \frac{1}{6\pi r\eta} \tag{19}$$

where B is the mobility of a hard spherical atom or ion of radius r moving in a continuous medium of viscosity η. Using the Nernst–Einstein equation:

$$D = BkT \tag{20}$$

where k is the Boltzmann constant, and T the thermodynamic temperature, gives the Stokes–Einstein equation relating D and η:

$$D = \frac{kT}{6\pi r\eta} \tag{21}$$

This model works well for simple liquids and molten salts, but for diffusion in silicate liquids gives ionic radii orders of magnitude too small.[94]

A similar approach has been used by Eyring and coworkers[95,96] assuming a simple liquid having crystal-like structure. Viscous flow and self-diffusion result from atoms jumping from one site to a hole, as illustrated in Fig. 8. The movement of the small sphere A (oxygen ion) of radius λ, through a distance πr, where r is the diameter of the large ion B (silicate anion), results in the transport of the B ion to the left, and gives:

$$D = \frac{kT}{\lambda\eta} \tag{22}$$

for the self-diffusion coefficient of the small ion. Diffusivities calculated from this model for a number of silicate liquids are in good agreement with the experimentally determined values.[90,94] In some cases, eqn (21) more accurately describes silicate melt diffusion if a larger diffusing ion than O^{2-} ($V_i = 9{\cdot}2 \times 10^{-30}\ m^3$), such as SiO_4^{4-} ($V_i = 1{\cdot}1 \times 10^{-28}\ m^3$), is assumed.[97] Schreiber *et al.*[99] have argued that some deviations from Eyring's model can be attributed to the wrong mechanism being assumed. If the measured diffusion rates are much higher than predicted it is likely that oxygen permeation through channels in the melt structure is occurring. Schaeffer has proposed that molecular oxygen permeation can assist oxygen self-diffusion in silicate glasses, in much the same as was proposed for silica glass.[100] Most workers consider oxygen permeation in liquid silicates to be by the molecule O_2.[99–101] Doremus,[102] however, observed that permeation rates in liquids were much higher than in silica glass provided O_2 dissociates into atomic oxygen (a smaller species), which diffuses at a higher rate.

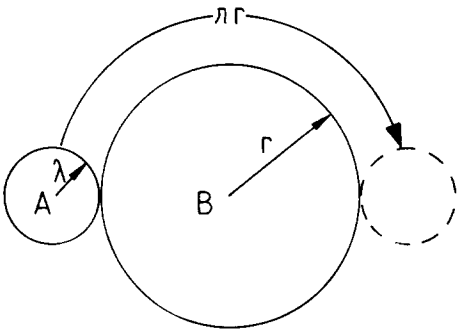

Fig. 8. Silicate glass diffusion model, after Eyring.[95,96]

An alternative mechanism has been proposed on the basis of work with liquid K_2O–SiO_2,[98] for which an observed $p_{O_2}^{-1/2}$ diffusion dependence was interpreted as implying a vacancy mechanism at non-bridging oxygen sites, described schematically:

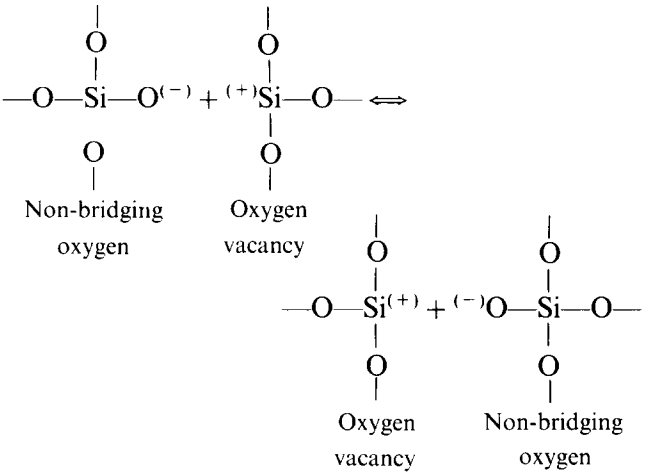

There is, however, disagreement in the literature as to the pressure dependence of oxygen diffusion in silicate liquids. A pressure dependence of $p_{O_2}^{1/2}$ has been determined for calcium aluminoborate liquids;[103] other investigations of soda–lime–silica glasses have shown no oxygen pressure dependence.[94]

4 Conclusions

The relevance of these data to the oxidation of silicon-based ceramics such as silicon carbide and

silicon nitride, in as far as the reaction rate is controlled at least partially by the migration of oxygen through a silica or silicate film, now remains to be assessed.

Oxidation requires the presence of an adequately high oxygen potential at the non-oxide interface. How this potential is maintained is not important, but the fastest oxygen transport process through the silica (or silicate) film at oxidation temperature in order to maintain the oxygen potential will be the one linked kinetically to the rate-controlling step. It is clear, as Fig. A1 shows, that over a wide temperature band oxygen migrates faster through non-crystalline silica as molecular oxygen, than by network self-diffusion. Although self-diffusion in silica glass appears to be greatly enhanced by dissolved molecular oxygen, the pure permeation process at temperatures of interest (900–1300°C) is still the fastest. The permeation rates of molecular oxygen through the crystalline forms of silicon dioxide have apparently not been measured; on the basis of a simple comparison of the self-diffusion coefficients for oxygen in the crystalline and amorphous forms of silica, the rate of oxygen transport by permeation might be expected, on balance, to be faster than by self-diffusion, and probably slower than that of oxygen permeation in amorphous silica. It is clear, however, that chemical purity is an important factor influencing oxygen self-diffusion and permeation.

There are only few published data for the permeation of molecular oxygen through silicate glasses at temperatures below θ_g. Partial blocking of the permeation channels by network modifying cations to the large O_2 (242 pm) molecules might be expected, possibly favouring migration of oxygen by network self-diffusion. Data suggest, however, that molecular permeation is still by far the fastest process. There is little if any discontinuity between the broad band of diffusion coefficient values measured for permeation in silicate materials above the glass transition temperatures and those below.

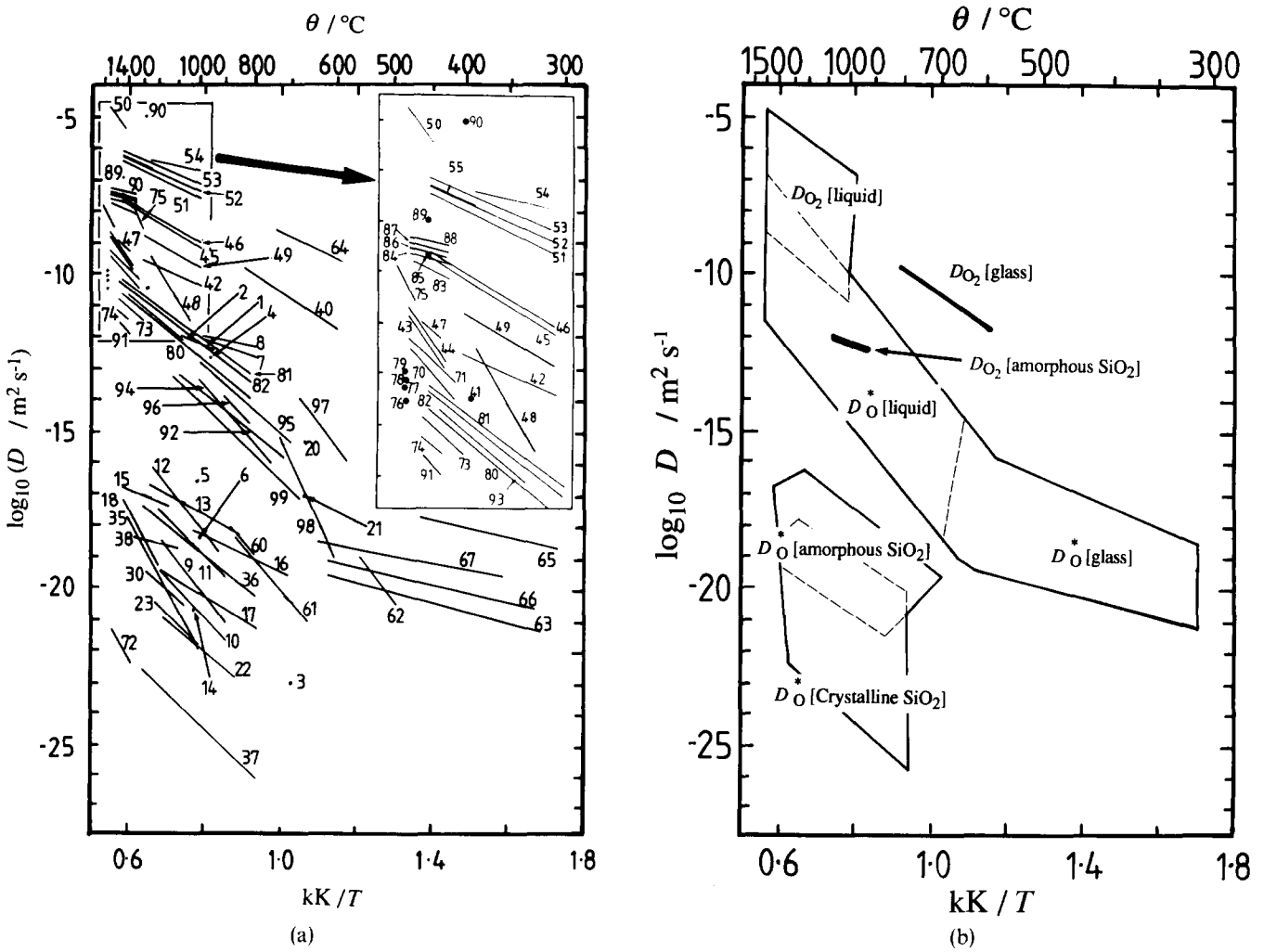

Fig. 9. Summary of literature oxygen diffusion behaviour in silicon dioxide and silica-based glasses. (a) Oxygen diffusion in silicon dioxide, silicate glasses and glass-forming liquids. (b) Oxygen diffusion in silicon dioxide, silicate glasses and liquids—broad overview of data.

Network oxygen self-diffusion in the silicate glasses is slower by several orders of magnitude than permeation. At higher temperatures the migration of oxygen through the liquid silicates by any route is very fast, because of the presence of high concentrations of 'network defects'. Compositional effects appear now to become more significant and some overlap of data for permeation and network diffusion is seen, though on balance permeation is still faster, though with some reservations regarding interpretation of data based on doubts about the oxygen pressure dependence. This subject clearly needs more investigation. The marked influence of bond breaking is seen in comparisons of permeation data for amorphous silicon dioxide and the liquid silicates. The weakening of the Si–O bonds with incorporation of the network modifying metal oxides is associated also with other physical and chemical changes, such as the lowering of viscosity and increased chemical reactivity generally.

It is clear that the transport of oxygen through a silica or silicate film on a silicon-based ceramic such as silicon carbide or silicon nitride occurs most rapidly as molecular oxygen. Conversion of a potentially protective silica film to a glassy or liquid silicate by reaction with gas-borne impurity metal oxides or salts, or with metal oxide diffusing outwards from the intergranular regions of a multiphase material, would be expected to lead to an increase in oxygen permeation rate by five or more orders of magnitude. For all these reasons the oxidative corrosion of silicon-based ceramics in the presence of silicate-forming components or fluxes becomes a very fast reaction indeed.

Acknowledgements

The authors would like to express their gratitude to Dr H. A. Schaeffer of the Deutsche Glastechnische Gesellschaft for originally stimulating interest in this subject, and for many subsequent very helpful discussions and comments. Dr E. Gilbart is thanked for computing assistance. Financial support was provided by the Commission of the European Communities through Stimulation Action Programme ST2J-0146-1-UK, and through EURAM Contract MA1E-0037-C(A).

References

1. Singhal, S. C., Thermodynamic analysis of the high-temperature stability of silicon nitride and silicon carbide. *Ceram. Int.*, **2**(3) (1976) 123–30.
2. Heuer, A. H. & Lou, V. L. K., Volatility diagrams for silica, silicon nitride, and silicon carbide and their application to high-temperature decomposition and oxidation. *J. Am. Ceram. Soc.*, **73**(10) (1990) 2785–3128.
3. Schlichting, J., Oxygen transport through silica surface layers on silicon containing ceramic materials. *High Temp.-High Pressures*, **14**(6) (1982) 717–24.
4a. Andrews, P. & Riley, F. L., The microstructure and composition of oxide films formed during high-temperature oxidation of a sintered silicon nitride. *J. Eur. Ceram. Soc.*, **5**(4) (1989) 245–56.
4b. Andrews, P. & Riley, F. L., Silicon nitride oxidation/reoxidation. *J. Eur. Ceram. Soc.*, **7**(2) (1991) 125–32.
5. Lamkin, M. A. & Riley, F. L., Oxidation resistant yttrium-containing silicon nitride. To be published.
6. Harrop, P. J., Self-diffusion in simple oxides (a bibliography). *J. Mater. Sci.*, **3**(2) (1968) 206–22.
7. Freer, R., Bibliography. Self-diffusion and impurity diffusion in oxides. *J. Mater. Sci.*, **15**(4) (1980) 803–24.
8. Freer, R., Diffusion in silicate minerals and glasses: A data digest and guide to the literature. *Contrib. Mineral. Petrol.*, **76**(4) (1981) 440–54.
9. Frischat, G. H., In *Ionic Diffusion in Oxide Glasses, Diffusion and Defect Monograph Series*, (3/4), Trans. Tech. Publications, 1975.
10. Sosnan, R. B., *The Phases of Silica*. Rutgers University Press, New Brunswick, NJ, 1965.
11. Lacy, E. D., Atomic packing in silicate glasses. In *The Vitreous State*. Glass Delegacy of the University of Sheffield, Sheffield, 1955, pp. 22–5.
12a. Bruckner, R., Properties and structure of vitreous silica. I. *J. Non-Cryst. Solids*, **5** (1970) 123–75.
12b. Bruckner, R., Properties and structure of vitreous silica. II. *J. Non-Cryst. Solids*, **5** (1970) 177–216.
13. Garofalini, S. H. & Miller, A. D., Kinetics of tridymite formation. *J. Cryst. Growth*, **78**(1) (1986) 85–96.
14. Buerger, M. J., Stuffed deviations of the silica structures. *Am. Mineral.*, **39**(7/8) (1954) 600–14.
15. Florke, O. W., Structural anomalies in tridymite and cristobalite. *Ber. Deut. Keram. Ges.*, **32**(12) (1955) 369–81; a review of this paper is given in English by Eitel, W., *Bull. Am. Ceram. Soc.*, **36**(4) (1957) 142–8.
16. Holmquist, S. B., Conversion of quartz to tridymite. *J. Am. Ceram. Soc.*, **44**(2) (1961) 82–6.
17. Hill, V. G. & Roy, R., Silica structure studies: V. The variable inversion in cristobalite. *J. Am. Ceram. Soc.*, **41**(12) (1958) 532–7.
18. Hill, V. G. & Roy, R., Silica structure studies: VI. On tridymite. *Trans. Brit. Ceram. Soc.*, **57**(8) (1958) 496–510.
19. Rockett, T. J. & Foster, W. R., The thermal stability of purified tridymite. *Am. Mineral*, **52**(7–8) (1967) 1233–40; discussed by Holmquist, S., *Am. Mineral.*, **53**(3–4) (1968) 501–3; reply by Foster, W. R., *Am. Mineral.*, **53**(3–4) (1968) 504–5.
20. Kerr, P. F., *Optical Mineralogy*, 4th edn. McGraw Hill, NY, 1977, pp. 272–85.
21. Mason, B. & Berry, L. G., *Elements of Mineralogy*. W. H. Freeman and Co., San Francisco, 1968, pp. 406–16.
22. Muehlenbachs, K. & Schaeffer, H. A., Oxygen diffusion in vitreous silica—utilization of natural isotopic abundances. *Can. Mineral.*, **15**(2) (1977) 179–84.
23. Revesz, A. G., Noncrystalline silicon dioxide films on silicon: A review. *J. Non-Cryst. Solids*, **11**(4) (1973) 309–30.
24. Zachariasen, W. H., The atomic arrangement in glass. *J. Am. Chem. Soc.*, **54**(10) (1932) 3841–51.
25. Warren, B. E. & Biscoe, J., Fourier analysis of X-ray patterns of soda–silica glass. *J. Am. Ceram. Soc.*, **21**(7) (1938) 259–65.

26. Revesz, A. G., A new model for defects in non-crystalline silicon dioxide. *J. Non-Cryst. Solids*, **4**(1) (1969) 347–56.
27. Revesz, A. G. & Schaeffer, H. A., The mechanism of oxygen diffusion in vitreous silica. *J. Electrochem. Soc.*, **129**(2) (1982) 357–61.
28. Revesz, A. G. & Hughes, H. L., The structure of thermally grown noncrystalline films on silicon. *J. Non-Cryst. Solids*, **71**(1–3) (1985) 87–94.
29. Revesz, A. G., Mrstik, B. J., Hughes, H. L. & McCarthy, D., Structure of SiO_2 films on silicon as revealed by oxygen transport. *J. Electrochem. Soc.*, **133**(3) (1986) 586–92.
30. Gibson, J. M. & Dong, D. W., Direct evidence for 1 nm pores in 'dry' thermal SiO_2 from high-resolution transmission electron microscopy. *J. Electrochem. Soc.*, **133**(3) (1986) 586–92.
31. Kreidl, N. J., Inorganic glass-forming systems. In *Glass: Science and Technology*, Vol. 1, ed. D. R. Uhlmann & N. J. Kreidl. Academic Press, NY, 1983, pp. 105–299.
32. Milberg, M. E. & Peters, C. R., Cation distribution in thallium silicate glasses. *Phys. Chem. Glasses*, **10**(2) (1969) 46–9.
33. Urnes, S., Studies of the sodium distribution in sodium glasses by the chemical difference method. *Phys. Chem. Glasses*, **10**(2) (1969) 69–71.
34. Grimshaw, R. W., Hargreaves, J. & Roberts, A. L., Kinetics of the quartz transformation. *Trans. Brit. Ceram. Soc.*, **55**(1) (1956) 36–56.
35. Rieck, G. D. & Stevels, J. M., The influence of some metal ions on the devitrification of glasses. *J. Soc. Glass Technol.*, **35** (1951) 284–8.
36. De Keyser, W. L. & Cypres, R., Contribution to the study on the formation of tridymite: combined action of lime and alkali oxide. *Silicates Industriels*, **25** (1960) 109–37.
37. De Keyser, W. L. & Cypres, R., The action of mineralizers on the crystallization of colloidal silica. *Silicates Industriels*, **26**(5) (1961) 237–43.
38. Coquerelle, M., Proposition for a mechanism for the formation of tridymite and cristobalite from a silica glass, based on diffusion and nucleation. *Silicates Industriels*, **26** (1961) 505–21.
39. Madden, G. I. & Van Vlack, L. H., Transformation of quartz to tridymite in the presence of binary silicate liquids. *J. Am. Ceram. Soc.*, **50**(8) (1967) 414–8.
40. Bassett, D. R., Boucher, E. A. & Zettlemoyer, A. C., The effect of alkali halides and silver nitrate on the crystallization of silica powders. *J. Mater. Sci.*, 7(12) (1972) 1379–82.
41. Austrheim, I., Cristobalite and tridymite crystallization in amorphous silica, collected from the smoke from silicon metal furnaces. *Trans. Brit. Ceram. Soc.*, **76**(6) (1977) 134–8.
42a. Norton, F. J., Permeation of gaseous oxygen through vitreous silica. *Nature*, **191**(4789) (1961) 701.
42b. Norton, F. J., Gas permeation through the vacuum envelope. In *Trans. Natl. Vacuum Symp. Am. Vacuum Soc.*, 1961, Vol. 8, 1962, pp. 8–16.
43. Haul, R., Dumbgen, G., Study of oxygen mobility in titanium dioxide, quartz, and quartz glass by means of heterogeneous isotope exchange. *Z. Elektrochem.*, **66**(8–9) (1962) 36–41.
44. Sucov, E. W., Diffusion of oxygen in vitreous silica. *J. Am. Ceram. Soc.*, **46**(1) (1963) 14–20.
45. Williams, E. L., Diffusion of oxygen in fused silica. *J. Am. Ceram. Soc.*, **48**(4) (1965) 190–4.
46. Yinnon, H., A proton activation study of oxygen diffusion in multicomponent glass-forming systems. PhD Thesis, Case Western Reserve University, Cleveland, Ohio, 1979.
47. Kalen, J. D., Boyce, R. S. & Cawley, J. D., Oxygen tracer diffusion in vitreous silica. *J. Am. Ceram. Soc.*, **74**(1) (1991) 203–9.
48. Cawley, J. D. & Boyce, R. S., A solution of the diffusion equation for double oxidation in dry oxygen including lazy exchange between network and interstitial oxygen. *Phil. Mag.*, **58A**(4) (1988) 589–601.
49. Mikkelsen, J. C., Self-diffusivity of network oxygen in vitreous SiO_2. *Appl. Phys. Lett.*, **45**(11) (1984) 1187–9.
50. Barrer, R. M., The mechanism of activated diffusion through the silica glass. *J. Chem. Soc.*, (1) (1934) 378–86.
51. Doremus, R. H., Oxidation of silicon by water and oxygen and diffusion in fused silica. *J. Phys. Chem.*, **80**(16) (1976) 1773–5.
52. Mott, N. F., Mechanisms for the oxidation of silicon and the formation of charged defects. *Proc. Roy. Soc., London*, **A376**(1765) (1981) 207–15.
53. Schaeffer, H. A. & Muehlenbachs, K., Correlations between oxygen transport phenomena in non-crystalline silica. *J. Mater. Sci.*, **13**(5) (1978) 1146–8.
54. Motzfeld, K., On the rates of oxidation of silicon and of silicon carbide in oxygen, and correlation with permeability of silica glass. *Acta Chem. Scand.*, **18**(7) (1964) 1596–606.
55. Deal, B. E. & Grove, A. S., General relationship for the thermal oxidation of silicon. *J. Appl. Phys.*, **36**(12) (1965) 3770–8.
56. Cristy, S. S. & Condon, J. B., A model for oxidation of silicon by oxygen. *J. Electrochem. Soc.*, **128**(10) (1981) 2170–4.
57. Costello, J. A. & Tressler, R. E., Isotope labelling studies of the oxidation of silicon at 1000 and 1300°C. *J. Electrochem. Soc.*, **131**(8) (1984) 1944–7.
58. Han, C. J. & Helms, C. R., Isotopic tracer studies of oxygen transport through SiO_2 films at 1000°C using secondary ion mass spectrometry. *J. Appl. Pys.*, **59**(5) (1986) 1767–9.
59. Kilner, J. A., New techniques for studying mass transport in oxides. *Mater. Sci. Forum*, **7** (1986) 205–22.
60. Cawley, J. D., Halloran, J. W. & Cooper, A. R., Oxygen-18 tracer study of the passive thermal oxidation of silicon. *Oxid. Metals*, **28**(1/2) (1987) 1–16.
61. Basu, S. N. & Halloran, J. W., Tracer isotope distribution in growing oxide scales. *Oxid. Metals*, **27**(3/4) (1987) 143–55.
62. Anderson, O. L. & Stuart, D. A., Calculation of activation energy of ionic conductivity in silica glasses by classical methods. *J. Am. Ceram. Soc.*, **37**(12) (1954) 573–80.
63. Doremus, R. H., *Glass Science*. Wiley, NY, 1973, pp. 121–45.
64. Schaeffer, H. A., Oxygen and silicon diffusion-controlled processes in vitreous silica. *J. Non-Cryst. Solids*, **38/39**(2) (1980) 545–50.
65. Revesz, A. G., Mrstik, B. J. & Hughes, H. L., On the mechanism of interaction between $^{18}O_2$ gas and noncrystalline SiO_2. *J. Electrochem. Soc.*, **134**(11) (1987) 2911–14.
66. Meyer, W. & Neldel, H., Relation between the energy constant E and the quantity constant a in the conductivity–temperature formula for oxide semiconductors. *Z. Tech. Phys.*, **18**(12) (1937) 588–93; *Physik. Z.*, **38**(23) (1937) 1014–19.
67. Winchell, P., The compensation law for diffusion in silicates. *High Temp. Sci.*, **1**(2) (1969) 200–15.
68. Galwey, A. K., Compensation effect in heterogenous catalysis. *Adv. Catal.*, **26** (1977) 247–322.
69. Almond, D. P. & West, A. R., Entropy effects in ionic conductivity. *Solid State Ionics*, **18/19**(2) (1986) 1105–9.
70. Dyre, J. C., A phenomenological model for the Meyer–Neldel rule. *J. Phys.*, **C19**(27) (1986) 5655–64.
71. Dosdale, T. & Brook, R. J., Cationic conduction and diffusion and the compensation law. *J. Mater. Sci.*, **13**(1) (1978) 167–72.
72. Dosdale, T. & Brook, R. J., The relationship between measured activation enthalpy and pre-exponential factor:

rate processes in ionic crystals in the intrinsic–extrinsic region. *Solid State Ionics*, **8**(4) (1983) 297–304.
73. Dosdale, T. & Brook, R. J., Comparison of diffusion data and of activation energies. *J. Am. Ceram. Soc.*, **66**(6) (1983) 392–5.
74. Freer, R. & Dennis, P. F., Oxygen diffusion studies. I. A preliminary ion microprobe investigation of oxygen diffusion in some rock-forming minerals. *Mineral. Mag.*, **45**(337) (1982) 179–92.
75. Giletti, B. J. & Yund, R. A., Oxygen diffusion in quartz. *J. Geophys. Res.*, **89**(B6) (1984) 4039–46.
76. Dennis, P. F., Oxygen self-diffusion in quartz under hydrothermal conditions. *J. Geophys. Res.*, **89**(B6) (1984) 4047–57.
77. Elphick, S. C., Dennis, P. F. & Graham, C. H., An experimental study of the diffusion of oxygen in quartz and albite using an overgrowth technique. *Contrib. Mineral. Petrol.*, **92**(3) (1986) 322–30.
78. Schachtner, R. & Sockel, H. G., Study of oxygen diffusion in quartz by activation analysis. In *Reactivity of Solids, Proc. Int. Symp. (8th)*, ed. J. Wood, O. Lindquist, C. Helgeson, & N. G. Vannerburg. Plenum Press, NY, 1977, pp. 605–9.
79. Bremen, W., Naoumidis, A. & Nickel, H., Oxidation behaviour of pyrolytically deposited β-SiC under atmospheres of CO–CO_2-mixtures. *J. Nucl. Mater.*, **71**(1) (1977) 56–64.
80. Lee, H.-L., Choi, T.-W. & Kim, J.-W., Oxidation mechanism of Si_3N_4. *Yo Op Hoe Chi*, **17**(4) (1980) 197–202.
81. Choi, T.-W. & Lee, H.-L., Oxidation mechanism of SiC. *Yo Op Hoe Chi*, **18**(2) (1981) 79–82.
82. Barrer, R. M. & Vaughan, D. E., Solution and diffusion of helium and neon in tridymite and cristobalite. *Trans. Faraday Soc.*, **63**(9) (1967) 2275–90.
83. Beauchamp, E. K. & Walters, L. C., Helium and deuterium permeation through devitrified and fused silica. *Glass Technol.*, **11**(5) (1970) 139–43.
84. Shelby, J. E., Molecular diffusion in glasses and oxides. *Mater. Sci. Res.*, **9** (1975) 367–82.
85. Shelby, J. E., Helium migration in TiO_2–SiO_2 glasses. *J. Am. Ceram. Soc.*, **55**(4) (1972) 195–7.
86. Brandt, W. W. & Abe, M., Diffusion rates and solubilities of noble gases in silicate glasses as a function of SiO_2 content. In *Reactivity of Solids, Proc. Int. Symp. (7th)*, ed. J. S. Anderson, M. W. Roberts & F. S. Stone. Chapman and Hall, London, 1973, pp. 210–18.
87. Shelby, J. E., Effect of phase separation on helium migration in sodium silicate glasses. *J. Am. Ceram. Soc.*, **56**(5) (1973) 263–6.
88. Shelby, J. E., Helium diffusion and solubility in K_2O–SiO_2 glasses. *J. Am. Ceram. Soc.*, **57**(6) (1974) 260–3.
89. Rawal, B. S. & Cooper, A. R., Oxygen self-diffusion in a potassium strontium silicate glass using proton activation analysis. *J. Mater. Sci.*, **14**(6) (1979) 1425–32.
90. Yinnon, H. & Cooper, A. R., Oxygen diffusion in multicomponent glass forming silicates. *Phys. Chem. Glasses*, **21**(6) (1980) 204–11.
91. Schaeffer, H. A. & Oel, H. J., Oxygen-18-diffusion in lead glass. *Glastechn. Ber.*, **42**(12) (1969) 493–8.
92. Frank, W., Engell, H. J. & Seeger, A., Migration energy and solubility of oxygen in body-centred cubic iron. *Z. Metallkunde*, **58**(7) (1967) 452–5.
93. Lindemann, F. A., Molecular frequencies. *Phys. Z.*, **11** (1910) 609–12.
94. Oishi, Y., Terai, R. & Ueda, H., Oxygen diffusion in liquid silicates and relation to their viscosity. *Mater. Sci. Res.*, **9** (1974) 297–310.
95. Eyring, H., Viscosity, plasticity, and diffusion examples of absolute reaction rates. *J. Chem. Phys.*, **4**(4) (1936) 283–91.
96. Glasstone, S., Laidler, K. J. & Eyring, H., *The Theory of Rate Processes*, McGraw Hill, NY, 1941, Chapter 9, pp. 477–510.
97. Dunn, T., Oxygen diffusion in three silicate melts along the join diopside–anorthite. *Geochim. Cosmochim. Acta*, **46**(11) (1982) 2293–9.
98. May, H. B., Lauder, I. & Wollast, R., Oxygen diffusion coefficients in alkali silicates. *J. Am. Ceram. Soc.*, **57**(5) (1974) 197–200.
99. Schreiber, H. D., Kozak, S. J., Fritchman, A. L., Goldman, D. S. & Schaeffer, H. A., Redox kinetics and oxygen diffusion in a borosilicate melt. *Phys. Chem. Glasses*, **27**(4) (1986) 152–77.
100. Schaeffer, H. A., Structure–property relationships of the vitreous state. In *Progress in Nitrogen Ceramics*, ed. F. L. Riley. NATO ASI Series E, No. 65, Martinus Nijhoff, The Hague, Netherlands, 1983, pp. 303–21.
101. Sasabe, M. & Goto, K. S., Permability, diffusivity, and solubility of oxygen gas in liquid slag. *Metall. Trans.*, **5**(10) (1974) 2225–33.
102. Doremus, R. H., Diffusion of oxygen from contracting bubbles in molten glass. *J. Am. Ceram. Soc.*, **43**(12) (1960) 655–61.
103. Hagel, W. C. & MacKenzie, J. D., Electrical conduction and oxygen diffusion in aluminoborate and aluminosilicate glasses. *Phys. Chem. Glasses*, **5**(4) (1964) 113–19.
104. Susa, M., Shinohara, H., Nagata, K. & Goto, K. S., Diffusion of oxygen molecules in amorphous silica thin films. *J. Japan. Inst. Mat.*, **54**(2) (1990) 193–200.
105. Choudhury, A., Palmer, D. W., Amsel, G., Curien, H. & Baruch, P., Study of oxygen diffusion in quartz by using the nuclear reaction $O^{18}(p,\alpha)N^{15}$. *Solid State Commun.*, **3**(6) (1965) 119–22.
106. Goldman, D. S. & Gupta, P. K., Diffusion-controlled redox kinetics in a glassmelt. *J. Am. Ceram. Soc.*, **66**(3) (1983) 188–90.
107. Greene, C. H. & Kitano, I., Rate of solution of oxygen bubbles in commercial glasses. *Glastechn. Ber.*, **32**(5) (1959) 44–8.
108. Koros, P. J. & King, T. B., The self-diffusion of oxygen in a lime–silica–alumina slag. *Trans. Metall. Soc. AIME*, **224**(4) (1962) 299–306.
109. Lawless, W. N. & Wedding, B., Photometric study of the oxygen diffusivity in an aluminosilicate glass. *J. Appl. Phys.*, **41**(5) (1970) 1926–9.
110. Semkow, K. W. & Haskin, L. A., Concentrations and behaviour of oxygen and oxide ion in melts of composition $CaO.MgO.xSiO_2$. *Geochim Cosmochim. Acta*, **49**(9) (1985) 1897–908.
111. Kingery, W. D. & Lecron, J. A., Oxygen mobility in two silicate glasses. *Phys. Chem. Glasses*, **1**(3) (1960) 87–9.
112. Ueda, H. & Oishi, Y., Self-diffusion coefficients of oxygen in molten CaO–Al_2O_3–SiO_2-system glasses. *Asahi Garasu Kogyo Gijutsu Shoreikai Kenkyu Hokoku*, **16** (1970) 201–20.
113. Oishi, Y., Ueda, H. & Terai, R., Self-diffusion coefficient of oxygen and its relation to viscosity of molten silicates. In *Int. Congr. Glass, 10th*, Vol. 8, 1974, ed. Ceram. Soc. Jpn, 1974, pp. 30–5.
114. King, T. B. & Koros, P. J., Diffusion in liquid silicates. In *Kinetics of High Temperature Processes*, ed. W. D. Kingery. Wiley, NY, 1959, pp. 80–5.
115. Shiraishi, Y., Nagahama, H. & Ohta, H., Self-diffusion of oxygen in calcium oxide–silicon dioxide melt. *Can. Metall. Q.*, **22**(1) (1983) 37–43.
116. Keller, H., Schwerdtfeger, K., Petri, H., Holze, R. & Hennesen, K., Tracer diffusivity of O^{18} in CaO–SiO_2 melts at 1600°C. *Metall. Trans.*, **13B**(6) (1982) 237–40.
117. Terai, R. & Oishi, Y., Self diffusion of oxygen in soda-lime silicate glass. *Glastechn. Ber.*, **50**(4) (1977) 68–73.

118. Gaye, H. & Riboud, P., Diffusion coefficient of oxygen in $CaO–SiO_2$–iron oxides liquid system. *Circ. Inf. Tech., cent. Doc. Sider.*, **33**(1) (1976) 109–13.
119. Shimizu, N. & Kushiro, I., Diffusivity of oxygen in jadeite and diopside melts at high pressures. *Geochim Cosmochim. Acta*, **48**(6) (1984) 1295–303.
120. DiMarcello, F. V., Oxygen diffusion in a sodium silicate glass. Paper presented in the 68th Annual Meeting of the American Ceramic Society, Washington, 10 May 1966; abstract in *Am. Ceram. Soc. Bull.*, **45**(4) (1966) 420.
121. DeBerg, K. C. & Lauder, I., Oxygen tracer diffusion in a potassium silicate glass above the transformation temperature. *Phys. Chem. Glasses*, **21**(3) (1980) 106–9.
122. DeBerg, K. C. & Lauder, I., Oxygen tracer diffusion in lead silicate glass above the transformation temperature. *Phys. Chem. Glasses*, **19**(4) (1978) 78–82.
123. DeBerg, K. C. & Lauder, I., The diffusion of oxygen from water vapour–oxygen mixtures into lead silicate glass above the transformation temperature. *Phys. Chem. Glasses*, **19**(4) (1978) 83–8.

Appendix: Oxygen Mobility Data

Presented here are Tables A1–A4 and Figs A1–A4 showing published diffusion data for oxygen and cations of interest in this study. The data have largely been assembled using *Chemical Abstracts* and *Diffusion and Defect Data.*

Notation

cnq Composition not quoted
Hy Denotes experiments conducted in presence of significant amounts of water/hydrothermal conditions
Gl Glass—temperature below T_g
Me Melt/liquid—temperature above T_g
SC Single crystal

Method (for details see appropriate references from the data tables)

BC From the rate of contraction of gas bubbles in a melt
CE Capillary effusion
CR Capillary reservoir
EG Gas–solid exchange, mass spectrometric analysis of gas
ES Gas–solid exchange, mass spectrometric analysis of solid
GP Gas permeation
NP Oxygen profiling by a nuclear reaction
OC Deduced from the kinetics of silicon carbide oxidation
ON Deduced from the kinetics of silicon nitride oxidation
OS Deduced from the kinetics of the oxidation of silicon
OT Optical transmittance
PC Deduced from the change of pressure of diffusing gas
RB Rutherford back-scattered spectroscopy
RK Redox kinetics
SP Oxygen profiling by SIMS
TG Thermogravimetric analysis
UA Ultraviolet absorption on oxidation of reduced oxide

Table A1. Oxygen transport data in amorphous silicon dioxide

Number on Fig. A1	*Material*	*θ* (°C)	D_O ($m^2 s^{-1}$)	$\Delta H^{\ddagger}$ ($kJ mol^{-1}$)	*Method*	*Remarks*	*Refs*
Amorphous silica							
O_2 diffusion/permeation							
	—	680–944	—	131	GP	—	50
1	—	950–1 078	$2{\cdot}7 \times 10^{-8}$	113	GP	$D \propto p_{O_2}$	42
2	—	1 050	$D = 9{\cdot}7 \times 10^{-13}$	—	UA	—	103
3	Thermally grown	700	$D = 1 \times 10^{-23}$	—	OS	—	56
4	Thermally grown	960	$D = 2{\cdot}1 \times 10^{-13}$	—	OS	—	60
5	Thermally grown	1 000	$D = 2{\cdot}3 \times 10^{-17}$	—	OS	$D \propto p_{O_2}$	55
6	Thermally grown	1 000	$D = 4 \times 10^{-19}$	—	OS	—	57
7	CVD silica	800–1 000	$2{\cdot}22 \times 10^{-9}$	83	OS	—	104
8	Spin-on silica films	800–1 000	$3{\cdot}3 \times 10^{-9}$	60	OS	—	104
	Thermally grown and sputtered films	800–1 000	—	113	OS	—	104
9	Thermally grown	900–1 200	$2{\cdot}75 \times 10^{-9}$	280	OS SP	SiO_2–O_2 interface	48
10	Thermally grown	900–1 200	$1{\cdot}33 \times 10^{-11}$	241	OS SP	Si–SiO_2 interface	48
	Thermally grown	—	—	210	OS	20 nm layer	28
	Thermally grown	—	—	120	OS	~120 nm	28
	Thermally grown	—	—	90	OS	300 nm	28
Permeation-assisted self-diffusion							
11	Type I	900–1 200	$4{\cdot}3 \times 10^{-10}$	230	EG	—	43
12	—	925–1 225	$1{\cdot}51 \times 10^{-6}$	298	EG	—	44
13	—	850–1 250	$2{\cdot}10 \times 10^{-13}$	121	EG	—	45
14	—	1 012	$D = 2{\cdot}3 \times 10^{-21}$	—	EG	—	22
15	Type II	1 150–1 430	$4{\cdot}4 \times 10^{-15}$	82·5	ES	—	22
16	—	706–1 018	$2{\cdot}13 \times 10^{-14}$	111	NP	—	46
17	Thermally grown	800–1 200	$5{\cdot}54 \times 10^{-15}$	143	SP	—	47
Self-diffusion							
18	CVD	1 200–1 400	$2{\cdot}6 \times 10^{-4}$	450	SP	Thin film	49

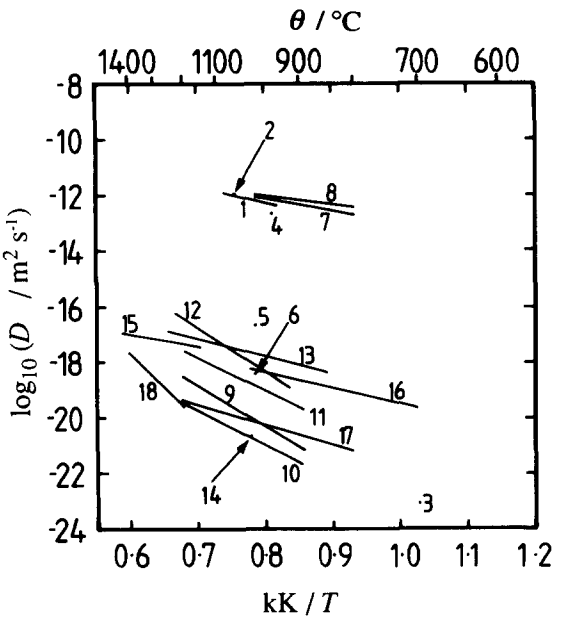

Fig. A1. Oxygen transport in amorphous silicon dioxide.

Table A2. Oxygen transport data in crystalline silicon dioxide

Number on Fig. A2	*Material*	*θ (°C)*	*D_O ($m^2 s^{-1}$)*	*$\Delta H^{\ddagger}$ ($kJ mol^{-1}$)*	*Method*	*Remarks*	*Refs*
Quartz							
Self-diffusion by ^{18}O gas/exchange							
20	β-$\parallel$c	667	$D = 4{\cdot}1 \times 10^{-16}$	—	NP	SC	105
21	β-$\perp$ (10$\bar{1}$0)	667	$D = 8{\cdot}1 \times 10^{-18}$	—	NP	SC	105
22	β	870–1 180	$1{\cdot}1 \times 10^{-14}$	195	NP	SC	78
23	β	1 010–1 220	$3{\cdot}7 \times 10^{-13}$	230	EG	—	43
Tridymite							
Self-diffusion							
30	—	1 070–1 280	$1{\cdot}1 \times 10^{-13}$	195	NP	—	78
Cristobalite							
Oxidation							
35	SiC	1 000–1 400	$4{\cdot}6 \times 10^{-5}$	430	OC	—	79
36	Powdered Si_3N_4	800–1 300	$6{\cdot}61 \times 10^{-12}$	187	ON	—	80
37	Partially sintered Si_3N_4	800–1 300	$4{\cdot}57 \times 10^{-16}$	221	ON	—	80
38	Powdered SiC	1 100–1 350	$3{\cdot}84 \times 10^{-17}$	61·5	OC	—	81

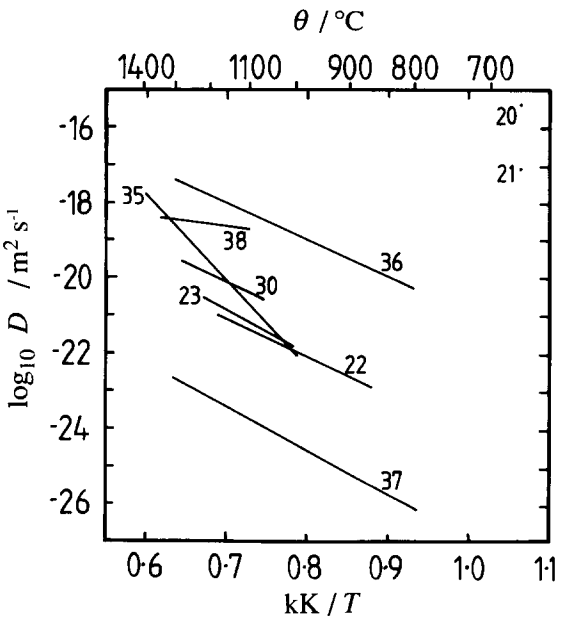

Fig. A2. Oxygen transport in crystalline silicon dioxide.

Table A3. Oxygen diffusion data for silicate glasses and liquids

Number on Fig. A3	*Composition (mol%)*	*Gl/Me*	*θ (°C)*	*D_O ($m^2 s^{-1}$)*	*$\Delta H^{\ddagger}$ ($kJ mol^{-1}$)*	*Method*	*Remarks*	*Refs*
O_2 permeation								
SiO_2–Al_2O_3–B_2O_3–CaO								
41	28·6–16·8–9·8–44·8	Me	1 260	$D = 3{\cdot}7 \times 10^{-11}$	—	RK	—	106
SiO_2–Al_2O_3–BaO–Sb_2O_3								
42	cnq	Me	1 000–1 300	$5{\cdot}4 \times 10^{-7}$	100	BC	—	108
SiO_2–Al_2O_3–CaO								
43	42·3–12·45–45·25	Me	1 372–1 535	$3{\cdot}73 \times 10^{1}$	360	CE	^{17}O tracer	108
44	42·3–12·45–45·25	Me	1 372–1 535	469×10^{1}	360	CE	^{18}O tracer	108
45	65–10–25	Me	1 000–1 450	$4{\cdot}5 \times 10^{-4}$	142	GP	—	101
46	40–15–45	Me	1 000–1 450	$4{\cdot}5 \times 10^{-4}$	136	GP	—	101
SiO_2–Al_2O_3–SrO–TiO_2								
40	39–2–30–29	Gl	630–830	$2{\cdot}84 \times 10^{-3}$	154	OT	—	108
SiO_2–As_2O_3–CaO–Na_2O–Sb_2O_3								
47	cnq	Me	1 396–1 473	$4{\cdot}2 \times 10^{-3}$	220	BC	—	92
SiO_2–Li_2O–Na_2O–TiO_2–ZrO_2 + 1%B_2O_3, La_2O_3, MgO								
48	56–12–3–17–11	Me	1 050–1 250	$6{\cdot}6 \times 10^{3}$	388	RK	—	99
Borosilicate + As_2O_3								
49	cnq	Me	1 000–1 300	$3{\cdot}2 \times 10^{-5}$	130	BC	—	107[a]
MgO.CaO.$2SiO_2$, diopside								
50	—	Me	1 425–1 550	$5{\cdot}42 \times 10^{4}$	330	EC	—	110
SiO_2–PbO								
51	30–70	Me	1 000–1 450	$8{\cdot}3 \times 10^{-4}$	110	GP	—	101
52	20–80	Me	1 000–1 450	$8{\cdot}3 \times 10^{-4}$	105	GP	—	101
53	10–90	Me	1 000–1 450	$8{\cdot}3 \times 10^{-4}$	100	GP	—	101
SiO_2–PbO–FeO								
54	12–>83–<5	Me	1 000–1 250	$2{\cdot}1 \times 10^{-5}$	50·2	GP	—	101
55	12–>83–<5	Me	1 250–1 450	$8{\cdot}3 \times 10^{-4}$	105	GP	—	101

[a] Calculated by [102].

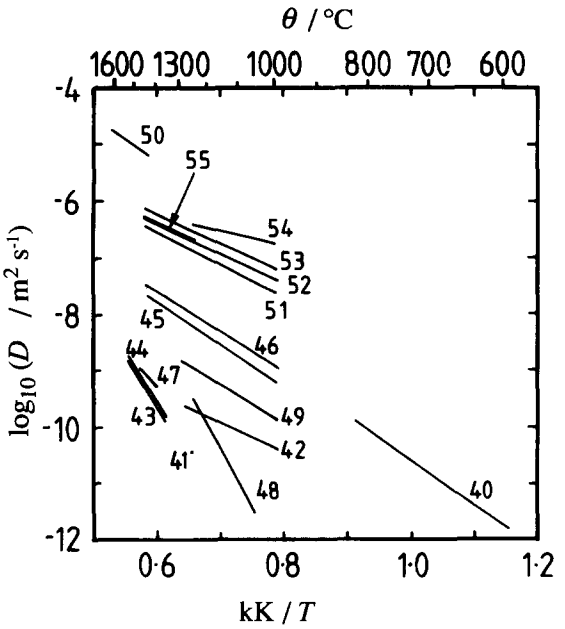

Fig. A3. Molecular oxygen self-diffusion in silicate glasses and glass-forming liquids.

Table A4. Oxygen self-diffusion data for silicate glasses and liquids

Number on Fig. A4	*Composition (mol%)*	*Gl/Me*	*θ (°C)*	D_O ($m^2 s^{-1}$)	$\Delta H^{\ddagger}$ ($kJ mol^{-1}$)	*Method*	*Remarks*	*Refs*
Oxygen self-diffusion								
SiO_2–Al_2O_3–CaO								
60	42·3–12·4–45·3	Gl	765–845	$7{\cdot}49 \times 10^{-7}$	255	EG	—	111
61	41·7–13·3–45·0	Gl	625–830	$2{\cdot}79 \times 10^{-7}$	245	EG	—	103
70	42·3–12·4–45·3	Me	1 320–1 540	$9{\cdot}2 \times 10^{-3}$	257	—	—	112
71	42·3–12·4–45·3	Me	1 320–1 540	$1{\cdot}8 \times 10^{-3}$	227	EG	—	113
72	42·3–12·4–45·3	Me	1 370–1 520	4×10^{-10}	410	ES	—	114
SiO_2–Al_2O_3–CaO–MgO								
73	50–9–25–16	Me	1 297–1 475	$1{\cdot}35 \times 10^{-5}$	200	EG	—	97
74	50–13·5–25–11·5	Me	1 388–1 476	$1{\cdot}29 \times 10^{-6}$	180	EG	—	97
SiO_2–CaO								
75	44–56	Me	1 550–1 650	$1{\cdot}5 \times 10^{3}$	408	CE	—	115
76	63·4–36·6	Me	1 600	$D^* = 3{\cdot}1 \times 10^{-11}$	—	NP	—	116
77	58·3–41·7	Me	1600	$D^* = 5{\cdot}8 \times 10^{-11}$	—	NP	—	116
78	53·3–46·7	Me	1 600	$D^* = 8{\cdot}8 \times 10^{-11}$	—	NP	—	116
79	48·3–51·7	Me	1 600	$D^* = 1{\cdot}16 \times 10^{-11}$	—	NP	—	116
SiO_2–CaO–Na_2O								
62	~72–~12–~16	Gl	460–525	2×10^{-1}	278	EG	—	111
80	~72–~12–~16	Me	800–1 470	$7{\cdot}9 \times 10^{-6}$	186	EG	—	117
81	~72–~12–~16	Me	800–1 470	$4{\cdot}5 \times 10^{-6}$	162	EG	—	112
82	71·1–12·1–16·1	Me	800–1 470	$1{\cdot}2 \times 10^{-6}$	153	EG	—	112
SiO_2–CaO–Fe_2O_3								
83	54·8–31·6–13·6	Me	1 350–1 550	$D_{1450} = 1{\cdot}15 \times 10^{-8}$	106	TG	—	118
84	51·0–29·4–19·6	Me	1 350–1 550	$D_{1450} = 1{\cdot}7 \times 10^{-8}$	55·6	TG	—	118
85	45·4–46·3–8·3	Me	1 350–1 550	$D_{1450} = 1{\cdot}85 \times 10^{-8}$	—	TG	—	118
86	43·0–43·5–13·5	Me	1 350–1 550	$D_{1450} = 2{\cdot}4 \times 10^{-8}$	46·0	TG	—	118
87	40·2–40·3–19·5	Me	1 350–1 550	$D_{1450} = 3{\cdot}2 \times 10^{-8}$	57·3	TG	—	118
88	30·9–49·7–19·4	Me	1 350–1 550	$D_{1450} = 3{\cdot}9 \times 10^{-8}$	48·5	TG	—	118
89	7·1–55·8–37·1	Me	1 350–1 550	$D_{1450} = 1{\cdot}04 \times 10^{-7}$	—	TG	—	118
CaO . MgO . $2SiO_2$, diopside								
90	—	Me	1 293	$D^* = 9{\cdot}1 \times 10^{-6}$	260	SP	—	119
91	—	Me	1 396–1 473	$1{\cdot}64 \times 10^{-4}$	260	EG	—	97
SiO_2–CaO–MgO–Na_2O								
63	71·5–9·3–6·1–13·1	Gl	290–580	$9{\cdot}1 \times 10^{-17}$	57·8	NP	—	90
92	71·5–9·3–6·1–13·1	Me	700–1 083	$6{\cdot}3 \times 10^{-6}$	208	NP	—	90
SiO_2–Na_2O								
64	86·9–13·1	Gl	550–700	5×10^{-14}	100	EG	—	120
93	80·5–19·5	Me	1 061–1 395	$2{\cdot}4 \times 10^{-5}$	192	EG	—	112
SiO_2–K_2O								
94	82·5–17·5	Me	750–1 000	$4{\cdot}0 \times 10^{-3}$	266	EG	—	98
95	73·6–26·4	Me	700–1 000	$2{\cdot}4 \times 10^{-5}$	199	EG	—	98
96	72·4–27·6	Me	820–902	$1{\cdot}7 \times 10^{-3}$	250	EG	$D^* \propto p_{O_2}$	121
SiO_2–K_2O–PbO								
65	53·4–8·7–33·0	Gl	275–425	1×10^{-14}	50	ES	—	91
97	53·4–8·7–33·0	Me	578–678	$3{\cdot}2 \times 10^{2}$	300	EG	$D^* \propto p_{O_2}$	122
SiO_2–K_2O–SrO								
66	71·1–15·1–13·8	Gl	295–580	$9{\cdot}3 \times 10^{-17}$	50·6	NP	—	90
67	71·1–15·1–13·8	Gl	327–600	1×10^{-16}	42	NP	—	89
98	71·1–15·1–13.8	Me	~600–727	$7{\cdot}6 \times 10^{10}$	498	NP	—	89
99	71·1–15·1–13·8	Me	680–1 121	$8{\cdot}5 \times 10^{-6}$	219	NP	—	90

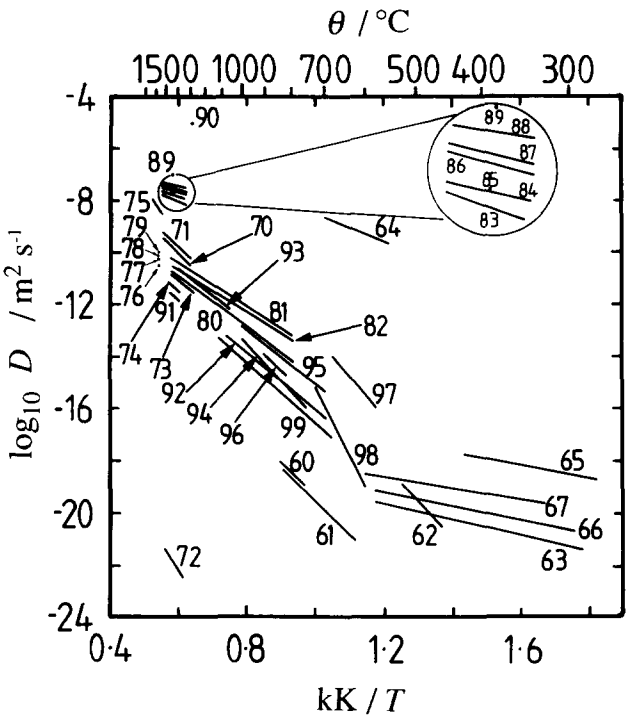

Fig. A4. Oxygen self-diffusion in silicate glasses and glass-forming liquids.